INTEGRATION FAULT DETECTION AND TOLERANT CONTROL IN MICRO-SATELLITE ATTITUDE PROPULSION MODE APPLICATION

Ho-Nien Shou
Department of Aviation & Communication Electronics, Air Force Institute of Technology, Kaohsiung, Taiwan, R.O.C.
E-mail: honien.shou@gmail.com

ICETI-2014, P1042_SCI
No. 15-CSME-51, E.I.C. Accession 3826

ABSTRACT

The paper refers to a tolerant control method which is reconfigurable to micro-satellites when they are out of order. The integrated approach to the design of thruster control reconfigurable fault-tolerant control system is proposed. The scheme includes a control effectiveness factor and a reconfigurable fault-tolerant controller. The fault detection, diagnosis and controller reconfiguration are carried out using the control effectiveness factor based on the information from a two-stage Kalman filter. By using the two-stage Kalman filter and digital controller, the nonlinear plant will be discretized. We present sufficient conditions under which a discrete-time controller that input-to-state stabilizes an approximate discrete-time model of a nonlinear plant with disturbances. The result shows the method enables us to solve the system faults and meet the requirement when there is a fault in the micro-satellites attitude control system.

Keywords: tolerant control; attitude control; two-stage Kalman filter; input-to-state stabilize.

DÉTECTION DES DÉFAILLANCES D'INTÉGRATION ET DU CONTRÔLE DE TOLÉRANCE DANS L'APPLICATION EN MODE D'ATTITUDE DE PROPULSION D'UN MICROSATELLITE

RÉSUMÉ

L'objet de cette étude est une méthode de contrôle de tolérance qui est reconfigurable pour des microsatellites quand ils sont hors d'usage. Une approche intégrée pour la conception de la reconfiguration d'un système de commande de tolérance aux défaillances est proposée. Le plan inclus un facteur d'efficacité des contrôles et un contrôleur reconfigurable de tolérance aux défaillances. La détection de défaillance, de diagnostic et la reconfiguration du contrôleur sont effectuées en se basant sur l'information à l'aide d'un filtre Kalman à deux étages. L'utilisation de ce filtre et d'un contrôleur digital et l'installation nonlinéraire est discréditée. Nous présentons des conditions suffisantes sous lesquelles un contrôleur en temps discret, que l'état d'entrée stabilise, un modèle approximatif de temps discret d'une installation nonlinéaire avec perturbation. Les résultats démontrent que la méthode nous permet de trouver une solution aux défaillances du système et rencontrer les conditions requises quand il y a une défaillance dans le système de commande d'attitude du minisatellite.

Mots-clés : commande de tolérance; commande d'attitude; filtre Kalman à deux étages.

1. INTRODUCTION

When the micro-satellites are conducting formation, orbit transfer, de-dumbing and attitude control, they need to use the thruster control to complete the task. The attitude sensors, actuators, thruster nuzzles and other components constantly perform various control operations. Therefore, if a fault occurs, the pressure control system, which carries out the above tasks, will cause the microsatellite to not complete the task. So, fault diagnosis and fault-tolerant control of satellite attitude control system in the aerospace area have become hot research topics as well as urgent problems requiring critical attention.

Meanwhile, the mechanism movement, fuel consumption and mission environmental impact will lead to unknown changes in the system model parameters of orbiting satellites, the attitude control technology, traditionally based on the exact model of fault-tolerant, has some limitations.

Considering the presence of various noises in microsatellite thrust control tasks, the unknown disturbance, model uncertainty, and the introduction of robust control sense, we propose an integrity passive fault tolerant control design method with a nonlinear uncertain system.

Fault diagnosis aspect uses two-stage Kalman filters algorithm designed to diagnose the fault type [1]. As a fault is diagnosed, the fault-tolerant control is used to accommodate this failure. The two-stage Kalman filtering algorithm is developed to estimate the size of control effectiveness factor in the closed-loop attitude control system. From the size of the control effectiveness factor, a statistical hypothesis test is developed to replace the fault detection and diagnosis (FDD) frame to diagnose whether any fault has happened [2]. Then, a reconfiguration fault-tolerant controller is utilized to compensate the primary controller by using the size of control effectiveness factor if some fault has indeed happened.

In the case of nonlinear sampled-data systems with disturbances, we present sufficient conditions under which a discrete-time controller that input-to-state stabilizes. An approximate discrete-time model of a nonlinear plant with disturbances would also input-to-state stabilize the exact discrete-time plant model in an appropriate sense [3, 4].

The remainder of this paper is organized as follows: Section 2 describes the problem formulation of microsatellite propulsion fault detection and tolerant control; Section 3 briefly introduces the nonlinear sampled-data system of the disturbance mathematical model; Section 4 legends the reconfigurable control stage, reconfigurable controller design; a simulation result description is provided in Section 5; and Section 6 offers the conclusion.

2. PROBLEM FORMULATION

2.1. Quaternion Attitude Description [5]

The quaternion described satellite attitude is composed of one scalar part and three vector parts, defined as

$$q = q_0 + q_1 i + q_2 j + q_3 k = \begin{bmatrix} q_0 & \mathbf{q}^T \end{bmatrix} \tag{1}$$

where q_0 is the quaternion scalar part, $\mathbf{q}$ is the vector part, and the four parameters meet the following constraint condition:

$$\sum_{i=0}^{3} q_i^2 = 1 \tag{2}$$

Therefore, only three of the four variables of quaternion are independent. According to Euler's rotation and quaternion definition, the attitude between orbit and satellite body system is described by quaternion. The attitude rotation matrix corresponding to orbit system to satellite body system is

$$C_o^b = \begin{bmatrix} 1-2\left(q_2^2+q_3^2\right) & 2\left(q_1q_2+q_0q_3\right) & 2\left(q_1q_3-q_0q_2\right) \\ 2\left(q_1q_2-q_0q_3\right) & 1-2\left(q_1^2+q_3^2\right) & 2\left(q_2q_3+q_0q_1\right) \\ 2\left(q_1q_3+q_0q_2\right) & 2\left(q_2q_3-q_0q_1\right) & 1-2\left(q_1^2+q_2^2\right) \end{bmatrix} \tag{3}$$

Note: the quaternion attitude matrix consists of quadratic term of quaternion $\mathbf{q}$, so the quaternion $-q = [-q_0 \quad -\mathbf{q}^T]^T$ can obtain the attitude matrix shown in Eq. (3). The non-uniqueness of the quaternion is consistent with the non-uniqueness of the Euler axis/angle. For instance, if the Euler rotation angle is 0 and 2π, the corresponding quaternions are $\begin{bmatrix} 1 & 0 & 0 & 0 \end{bmatrix}^T$ and $\begin{bmatrix} -1 & 0 & 0 & 0 \end{bmatrix}^T$ respectively, but they represent the same attitude and the same rotation in physical significance. This paper uses the positive value of quaternion for calculation. When Eq. (3) is written in vector form, then

$$C_o^b = I_3 - q_0\mathbf{q}^\times + \left(\mathbf{q}^\times\right)^2 \quad \text{or} \quad C_o^b = \left(q_0^2 - \mathbf{q}^T\mathbf{q}\right) I_3 + 2\mathbf{q}\mathbf{q}^T - 2q_0\mathbf{q}^\times \tag{4}$$

where $\mathbf{q}^\times$ represents the skew symmetric matrix

$$\mathbf{q}^\times = \begin{bmatrix} 0 & -q_3 & q_2 \\ q_3 & 0 & -q_1 \\ -q_2 & q_1 & 0 \end{bmatrix} \tag{5}$$

2.2. Properties of Attitude Rotation Matrix

The attitude rotation matrix C_o^b, depicted by Eq. (3), can be expressed as

$$C_o^b = \begin{bmatrix} c_1 & c_2 & c_3 \end{bmatrix} \tag{6}$$

where $c_i = [c_{1i} \quad c_{2i} \quad c_{3i}]^T$, $i = 1,2,3$ represents the direct cosine vector. C_o^b is the orthogonal matrix, the properties are described below:

$$\begin{aligned} &C_o^b = (C_b^o)^{-1} = (C_b^o)^T, \quad c_1 \times c_2 = c_3, \quad c_2 \times c_3 = c_1, \quad c_3 \times c_1 = c_2, \\ &(c_{1i})^2 + (c_{2i})^2 + (c_{3i})^2 = 1 \quad \text{and} \quad (c_{j1})^2 + (c_{j2})^2 + (c_{j3})^2 = 1 \end{aligned} \tag{7}$$

The projection of the angular rate of the satellite body system in relation to the orbit system is defined as ω_{ob}^b. The following relationship can be deduced for the attitude of rotation: matrix C_o^b

$$\dot{C}_o^b = -C_o^b \left(\omega_{ob}^b\right)^\times, \quad \dot{c}_i = c_i \times \omega_{ob}^b = (c_i)^\times \omega_{ob}^b \tag{8}$$

The attitude of the microsatellite is represented in terms of quaternion $q = [q_0 \quad \mathbf{q}^T]^T$ and $\mathbf{q} = [q_1 \quad q_2 \quad q_3]^T$. The kinematics equation is described by

$$\begin{bmatrix} \dot{q}_0 \\ \dot{\mathbf{q}} \end{bmatrix} = \frac{1}{2} \begin{bmatrix} 0 & -\omega_{ob}^{bT} \\ \omega_{ob}^b & -\omega_{ob}^b\times \end{bmatrix} \begin{bmatrix} q_0 \\ q \end{bmatrix} = \frac{1}{2} \begin{bmatrix} -\omega_{ob}^{bT} q \\ (q_0 I + \mathrm{q}^\times)\, \omega_{ob}^b \end{bmatrix} \tag{9}$$

where ω_{ob}^b is the angular velocity of the body frame with respect to the orbit frame and

$$\omega_{ob}^b\times = \begin{bmatrix} 0 & -\omega_z & \omega_y \\ \omega_z & 0 & -\omega_x \\ -\omega_y & \omega_x & 0 \end{bmatrix}$$

is an opposing skew matrix corresponding to ω_{ob}^b.

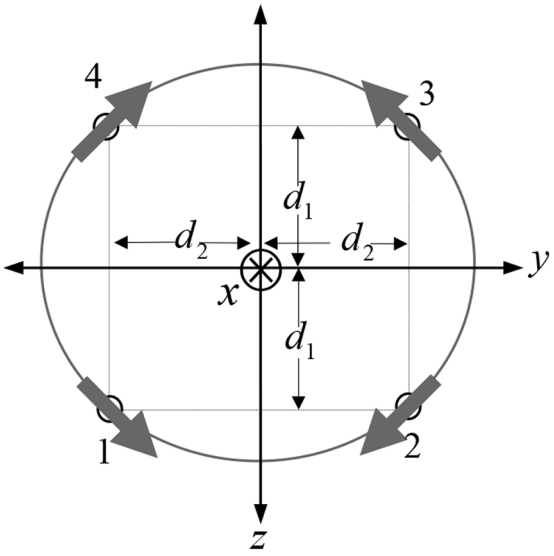

Fig. 1. Thrusting mounting geometry.

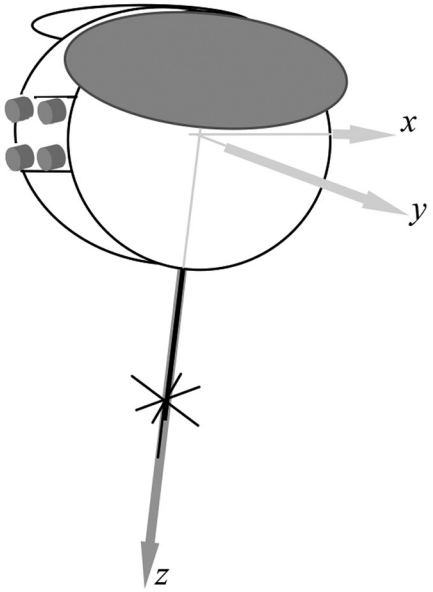

Fig. 2. Micro-satellite nominal on-orbit configuration.

2.3. Microsatellite Thrust-Torque Deduction [6]

The four thrusters of the spacecraft are mounted on the y–z plane of the satellite in each corner of a square. This is illustrated schematically in Fig. 1. The side length is $(d_1 + d_2 + \Delta d_1 + \Delta d_2)$, Δd_1 and Δd_2 are thruster canted inaccuracy length in Fig. 1. The arrows in Fig. 2 indicate the direction of force generated by each thruster in the body y–z plane. A combination of thrusters 2 and 4 produce $+x$ torque, while 1 and 3 produce $-x$ torques. Other thruster combinations produce torque about the y and z axes. The thrusters point primarily along $+x$-body axis, but canted $\phi + \Delta\phi$ from the x-axis to produce moments about the x-axis, $\Delta\phi$ is thruster canted inaccuracy angle in Fig. 3.

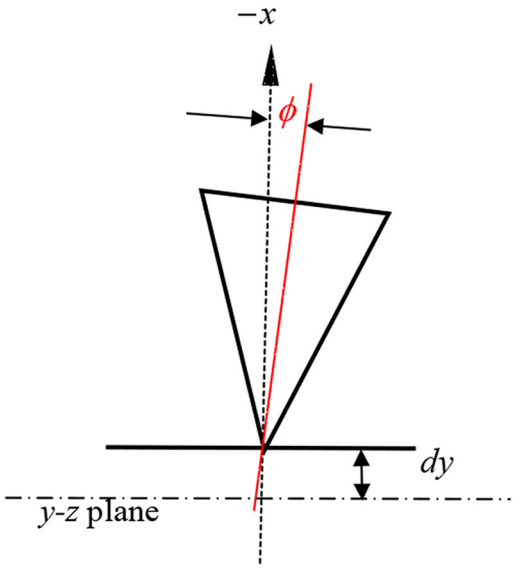

Fig. 3. Thruster mounting bias x-axis.

During thruster burning in attitude control, the momentum of the satellite changes rapidly. As fuel tank in the satellite geometry center, the function of center of mass (CM) offset dependent on the thrusters are mounted a distance with uncertainty. Since the thrusters are mounted at a distance l along the z-axis from the satellite center of mass (and coordinate system origin), the thrusters are canted such that the force vectors are 45° to the principle axes in the y–z plane.

For small ϕ, the thruster force can be rewritten as

$$\begin{bmatrix} \mathbf{F}_1 \\ \mathbf{F}_2 \\ \mathbf{F}_3 \\ \mathbf{F}_4 \end{bmatrix} = \begin{bmatrix} -1 & 1 & 1 \\ -1 & -1 & 1 \\ -1 & -1 & -1 \\ -1 & 1 & -1 \end{bmatrix} \begin{bmatrix} (1-\phi\Delta\phi)\,\mathbf{e}_x \\ \frac{d_1+\Delta d_1}{D}(\phi+\Delta\phi)\,\mathbf{e}_y \\ \frac{d_2+\Delta d_2}{D}(\phi+\Delta\phi)\,\mathbf{e}_z \end{bmatrix} \tag{10}$$

where $D = \sqrt{(d_1+\Delta d_1)^2 + (d_2+\Delta d_2)^2}$, and the resulting torque become

$$\tau_u^b = \begin{bmatrix} \tau_{u_x} \\ \tau_{u_y} \\ \tau_{u_z} \end{bmatrix} = \begin{bmatrix} \mathbf{r}_1\times\mathbf{F}_1 & \mathbf{r}_2\times\mathbf{F}_2 & \mathbf{r}_3\times\mathbf{F}_3 & \mathbf{r}_4\times\mathbf{F}_4 \end{bmatrix} \begin{bmatrix} u_1 \\ u_2 \\ u_3 \\ u_4 \end{bmatrix} = \begin{bmatrix} -\beta_1 & \beta_1 & -\beta_1 & \beta_1 \\ -\beta_2 & -\beta_2 & \beta_2 & \beta_2 \\ -\beta_3 & \beta_3 & \beta_3 & -\beta_3 \end{bmatrix} \begin{bmatrix} u_1 \\ u_2 \\ u_3 \\ u_4 \end{bmatrix} \tag{11}$$

where

$$\beta_1 = \frac{2d_1d_2}{\sqrt{d_1^2+d_2^2}}\phi, \quad \beta_2 = d_2 - \frac{d_2}{\sqrt{d_1^2+d_2^2}}l\phi, \quad \beta_3 = d_1 + \frac{d_1}{\sqrt{d_1^2+d_2^2}}l\phi,$$

$$\Delta\beta_1 = \frac{1}{\sqrt{d_1^2+d_2^2}}\left(2d_1d_2\Delta\phi + d_1\Delta d_2\phi + \Delta d_1 d_2\phi\right), \quad \Delta\beta_2 = \Delta d_2 - d_2\phi\Delta\phi - \frac{d_2}{\sqrt{d_1^2+d_2^2}}\left(l\Delta\phi + \Delta l\phi\right),$$

$$\Delta\beta_3 = \Delta d_1 - d_1\phi\Delta\phi + \frac{d_1}{\sqrt{d_1^2+d_2^2}}\left(l\Delta\phi + \Delta l\phi\right). \tag{12}$$

The variable τ_u^b is the control input, thruster command, which limited the nozzle saturation.

The dynamics of the spacecraft satellite is described by the equation of motion:

$$J\omega_{ib}^b = -\omega_{ib}^b \times J\omega_{ib}^b + \tau_d^b + \tau_u^b \tag{13}$$

where $J_0 + \Delta J$ is the moment of inertia matrix which is symmetric

$$J_0 + \Delta J = \begin{bmatrix} J_{xx} & 0 & 0 \\ 0 & J_{yy} & 0 \\ 0 & 0 & J_{zz} \end{bmatrix} + \begin{bmatrix} \Delta J_{xx} & 0 & 0 \\ 0 & \Delta J_{yy} & 0 \\ 0 & 0 & \Delta J_{zz} \end{bmatrix}$$

with J_{ii} being the moment of inertia along the i-axis and the ΔJ_{ii} being the associated uncertainty, τ_d^b is the disturbance torque input. The disturbing torque τ_d^b on the spacecraft may be attributed to gravity gradient, solar pressure, atmospheric drag and so on. The angular velocity ω_{ib}^b is the angular velocity of the body frame with respect to the inertial frame.

The angular velocity ω_{ib}^b can be expressed in the body frame as

$$\omega_{ib}^b = \omega_{io}^b + \omega_{ob}^b = C_o^b \omega_{ib}^o + \omega_{ob}^b \tag{14}$$

where C_o^b is given in Eq. (3) and $\omega_{io}^o = [0 \ -\omega_0 \ 0]^T$.

Since the orbit frame revolves to the inertial frame with the angular velocity of ω_0, by rearranging and differentiating the expression with respect to time, keeping in mind that $\omega_{io}^o$is constant, we obtain

$$\dot{\omega}_{ib}^b = \dot{\omega}_{ob}^b - \omega_{ob}^b \times C_o^b \omega_{io}^o \tag{15}$$

where the relation $\omega_{ob}^b = -\omega_{bo}^b$ is used. The dynamic equation for the microsatellite is now given as

$$\dot{\omega}_{ib}^b = J^{-1}\left[\left(-\omega_{ob}^b\times + C_o^b\omega_{io}^o\right)^\times J\left(-\omega_{ob}^b\times + C_o^b\omega_{io}^o\right)\right] + \omega_{ob}^b \times C_o^b\omega_{io}^o + J^{-1}\tau_d + J^{-1}\tau_u \tag{16}$$

With the new dynamical equation, the nonlinear state space model becomes

$$\begin{bmatrix} \dot{q}_0 \\ \dot{\mathbf{q}} \\ \dot{\omega}_{ob}^b \end{bmatrix} = \begin{bmatrix} -\frac{1}{2}\omega_{ob}^{bT} q \\ \frac{1}{2}\left(q_0 I + \mathrm{q}^\times\right)\omega_{ob}^b \\ J^{-1}\left[\left(-\omega_{ob}^b\times + C_o^b\omega_{io}^o\right)^\times J\left(-\omega_{ob}^b\times + C_o^b\omega_{io}^o\right)\right] + \omega_{ob}^b \times C_o^b\omega_{io}^o \end{bmatrix} + \begin{bmatrix} 0 \\ 0 \\ J^{-1} \end{bmatrix}\tau_d^b + \begin{bmatrix} 0 \\ 0 \\ J^{-1} \end{bmatrix}\tau_u^b \tag{17}$$

3. NONLINEAR SAMPLED-DATA SYSTEM

In the section, we will provide a framework for the design of stabilizing controllers via approximate discrete-time models for nonlinear sampled-data systems with disturbances. In particular, we present sufficient conditions under which a discrete-time controller that input-to-state stabilizes an approximate discrete-time model of a nonlinear plant with disturbances would also input-to-state stabilize (in an appropriate sense) the exact discrete-time plant model.

3.1. Dynamic Feedback Controllers

Consider a continuous-time nonlinear plant with disturbances

$$\dot{x}(t) = f(x(t), d(t), u(t)) \tag{18}$$

where $x \in \mathbb{R}^{n_x}$ is the state vector, $d \in \mathbb{R}^{p_1}$ is the disturbance and $u \in \mathbb{R}^{p_2}$ are respectively the state, exogenous disturbance and control input. It is assumed that f is locally Lipschitz and $f(0,0,0) = 0$. An equidistant grid on the time axis with a mesh $T = t_{k+1} - t_k > 0$ is considered, where $[t_k, t_{k+1}) = [kT, (k+1)T)$ is the sampling interval and T is the sampling period. It is assumed that system Eq. (18) is driven by an input that is piecewise constant over the sampling interval, i.e. the zero-order hold (ZOH) assumption holds true:

$$u(t) = u(kT) \equiv u_k = \text{constant}, \quad \text{for } kT < t < kT + T \tag{19}$$

The exact discrete-time model of (31) can be written as

$$x_{k+1} = x_k + \int_{kT}^{(k+1)T} (f(x(\tau)), d(\tau), u_k)\, d\tau \triangleq F_T^e(x_k, d_k, u_k) \tag{20}$$

where we assume that the disturbances $d(\bullet)$ are constant during sampling intervals, $d(t) = d[kT] = d_k$, $\forall\, t \in [kT, (k+1)T)$. We emphasize that F_T^e is not known in most cases. Indeed, in order to compute F_T^e we have to solve the initial value problem (20) analytically and this is usually impossible since f in (18) is nonlinear.

Hence, we will use an approximate discrete-time model of the plant to design a controller.

The corresponding approximate discrete-time model can be written as

$$x[k+1] = F_T^a(f(x_k), d_k, u_k) \tag{21}$$

The sampling period T is assumed to be a design parameter which can be arbitrarily assigned. Since we are dealing with a family of approximate discrete-time models F_T^a, parameterized by T, in order to achieve a certain objective we need, in general, to obtain a family of controllers, parameterized by T.

We consider a family of dynamic feedback controllers:

$$z_{k+1} = G_T(x_k, z_k) \tag{22}$$

$$u_k = u(x_k, z_k) \tag{23}$$

where $z \in \mathbb{R}^{n_z}$. We let $\bar{x}_k = \left[x_k^T z_k^T\right]^T$, $\bar{x}_k \in \mathbb{R}^{n_{\bar{x}}}$, where $n_{\bar{x}} = n_x + n_z$ and

$$\mathbf{F}_T^i(x_k, d_k) = \begin{pmatrix} F_T^i(f(x_k), d_k, u(x_k, z_k)) \\ G_T(x_k, z_k) \end{pmatrix} \tag{24}$$

The superscript i may be either e or a, where e stands for exact model, a for approximate model. We omit the superscript if we refer to a general model.

3.2. Stability of Nonlinear Sampled-Data Systems

In this section, we state and prove the result from the section above. The results specify conditions on the approximate model, the controller and the plant, which guarantee that the family of controllers (G_T, u_k) that input-to-state stabilize F_T^a would also input-to-state stabilize F_T^e for an appropriate T.

Definition 1. The family of systems $\mathbf{F}_T^i(\bar{x}_k, u_k)$ is Lyapunov semiglobally practically input-to-state stable, if there exist functions $\alpha_1,\ \alpha_2,\ \alpha_3 \in \mathrm{K}_\infty$ and $\gamma \in \mathrm{K}$, and for any strictly positive-real numbers $(\Delta_1, \Delta_2, \delta_1, \delta_2)$ there exist strictly positive-real numbers T^* and L, such that for all $T \in (0, T^*)$ there exists a function $V_T : \mathbb{R}^{n_{\bar{x}}} \to \mathbb{R}_{\geq 0}$ such that for all $\bar{x}_k \in \mathbb{R}^{n_{\bar{x}}}$ with $|\bar{x}_k| \leq \Delta_1$ and all $d \in L_\infty$ with $\|d\|_\infty \in \Delta_2$ the following holds:

$$\alpha_1(|\bar{x}_k|) \leq V_T \leq \alpha_2(|\bar{x}_k|) \tag{25}$$

$$\frac{1}{T}\left(V_T\left(\mathbf{F}_T\left(\bar{x}_k,d_k\right)\right)-V_T\left(\bar{x}_k\right)\right)\leq\alpha_3\left(|\bar{x}_k|\right)+\gamma\left(\|d_k\|_\infty\right)+\delta_1 \tag{26}$$

and, moreover, for all x_1,x_2,z with $|(x_1^T,z^T)^T|$, $|(x_2^T,z^T)^T|\in[\delta_2,\Delta_1]$ and all $T\in(0,T^*)$, we have $|V_T(x_1,z)-V_T(x_2,z)|\leq L|x_1-x_2|$. The function V_T is called an input-to-state-stable Lyapunov function for the family $\mathbf{F}_T$.

Definition 2. The family of systems $\bar{x}_{k+1}=\mathrm{F}_T\left(\bar{x}_k,d_k\right)$ is semiglobal practical derivative input-to-state-stable if there exist $\beta\in\mathrm{K}L$and $\gamma\in\mathrm{K}_\infty$ such that for any strictly positive-real numbers $(\Delta_{\bar{x}},\Delta_d,\Delta_{\dot{d}},\delta)$ there exists $T^*>0$ such that for all $T\in(0,T^*)$,$|\bar{x}_k(0)|\leq\Delta_{\bar{x}}$ and all continuously differentiable $d(\bullet)$ such that $\|d\|_\infty\leq\Delta_d$, $\left\|\dot{d}\right\|_\infty\leq\Delta_{\dot{d}}$, the solutions of the family $\mathbf{F}_T$ satisfy $|\bar{x}_k|\leq\beta\left(|\bar{x}_k(0)|,kT\right)+\gamma\left(\|d\|_\infty\right)+\delta$, $\forall k\in\mathbb{N}$.

Theorem 1. Suppose that

(i) the family of approximate discrete-time models $\mathrm{F}_T^a\left(\bar{x}_k,\bullet\right)$ is Lyapunov semiglobally practically input-to-state-stable (where (33) is holds),

(ii) $\mathbf{F}_T^a$ is one-step weakly consistent with F_T^e, and

(iii) $u_T$is uniformly locally bounded. Then, the family of exact discrete-time models $\mathbf{F}_T^e\left(\bar{x},d_T\right)$ is semiglobal practical derivative input-to-state-stable.

The approximate DTD method is shown in Section 5. The example illustrates our main theorems and shows a quantitative advantage in using approximate DTD method over the CTD method.

4. RECONFIGURABLE CONTROL STRATEGY

In general, a reconfigurable FTCS consists of three parts: a reconfigurable controller, an FDD scheme, and a control law reconfiguration mechanism. In paper, the reconfigurable control laws and FDD scheme are designed separately. Ideally, at each step of the controller reconfiguration, the FDD scheme should provide information on the post-fault system in real time as precisely as possible, and the reconfigurable controller should be able to recover the performance of the pre-fault system to the maximum extent with consideration of the physical limitations of the system.

4.1. Control Effectiveness Factor Estimation [1]

$$\begin{aligned}x_{k+1}&=f\left(x_k\right)+g_2\left(x_k\right)\left(I-\Gamma_k\right)u_k+w_k^x\\ \gamma_{k+1}&=r_k\gamma_k+w_k^\gamma\\ z_k&=h\left(x_k\right)+v_k\end{aligned} \tag{27}$$

where x_k, u_k and z_k are the state, control input and output variables similar to the previous definition. w_k^x, w_k^γ and v_k are the process noise, effective factor noise and measurement noise, respectively. The noise sequences w_k^x, w_k^γ and v_k are assumed to be zero mean uncorrelated white Gaussian noise sequences with

$$E=\left\{\begin{bmatrix}w_i^x\\ w_i^\gamma\\ v_i\end{bmatrix}\begin{bmatrix}w_j^x & w_j^\gamma & v_j\end{bmatrix}\right\}=\begin{bmatrix}Q^x & 0 & 0\\ 0 & Q^\gamma & 0\\ 0 & 0 & R\end{bmatrix}\delta_{ij} \tag{28}$$

where $Q^x>0$, $Q^y>0$, $R>0$ and δ_{ij} is the Kronecker delta. Γ_k is a is a diagonal matrix with control effectiveness factor γ_k^i

$$\Gamma_k=\mathrm{diag}\left[\gamma_k^1,\gamma_k^2,\ldots\gamma_k^{p_2}\right],\quad \gamma_k^i=\begin{cases}1, & \text{normal}\\ 0, & \text{fault}\end{cases}\qquad \text{for } i=1,2,\ldots,p_2$$

and $\gamma_k = [\gamma_\gamma^1 \ \ \gamma_\gamma^2 \ \ \dots \ \ \gamma_\gamma^{p_2}]^T$, represents the partial loss in the control effectiveness of the ith actuator. The initial state $x_k(0)$ and $\gamma_k(0)$ are assumed to be uncorrelated with the white noise processes w_k^x, w_k^γ and v_k.

The FDD is carried out using online statistical hypothesis tests of the control effectiveness factor based on the information from a two-stage Kalman filter. If the results of statistical hypothesis tests show that there are faults in actuators, then the fault-tolerance controller can utilize the size of control effectiveness factor to reconfigure the primary controller. Consequently, this paper uses the statistical hypothesis tests to replace the FDD to diagnose whether there some fault has happened. The size of control effectiveness factor shows the size of fault.

4.2. Reconfigurable Controller Design [7]

Under unscented Kalman filter, the state variable x_k with mean $\tilde{x}_k$ and covariance P_k can be approximated by sigma points $\chi_{i,k}$ selected from the columns of$\tilde{x}_k \pm \left(a\sqrt{LP_k}\right)_i$, $i = 1,2,\dots,2L$. The opposite weight w_i is $w_0 = 1-(1/a^2)$, $w_i = 1/2La^2$ $(i = 1,2,\dots,2L)$.

The optimal two-stage Kalman estimator with random bias algorithm is described as follows:

$$\bar{\varepsilon}_k^b = z_k - z_k(-) - N_k\bar{b}_k \tag{29}$$

$$P_{zz}^b = E\left\{\bar{\varepsilon}_k^b\bar{\varepsilon}_k^{bT}\right\} = \sum_{i=0}^{2n} w_i\left(z_{i,k-1}(+) - z_k(-)\right)\left(z_{i,k-1}(+) - z_k(-)\right)^T + R_k + N_k\bar{P}_k^b(-)N_k^T \tag{30}$$

$$\bar{P}_{zz}^b = \frac{1}{M-1}\sum_{i=k-M+1}^{k}\bar{\varepsilon}_k^b\bar{\varepsilon}_k^{bT} \tag{31}$$

The bias filter is

$$\bar{u}_k(-) = r_{k-1}\bar{u}_{k-1}(+), \quad \bar{P}_k^{b*}(-) = \lambda_k^b\left(r_{k-1}\bar{P}_{k-1}^{b*}(+)\,r_{k-1}^T + \bar{Q}_{k-1}^b\right) \tag{32}$$

$$\bar{K}_k^{b*} = \bar{P}_k^{b*}(-)\left(\sum_{i=0}^{2n} w_i\left(z_{i,k-1}(+) - z_k(-)\right)\left(z_{i,k-1}(+) - z_k(-)\right)^T + R_k + N_k\bar{P}_k^{b*}(-)N_k^T\right)^{-1} \tag{33}$$

$$\bar{P}_k^{b*}(+) = \left(I - \bar{K}_k^{b*}N_k\right)\bar{P}_k^{b*}(-), \quad \bar{u}_k(+) = \bar{u}_{k-1}(-) + \bar{K}_k^{b*}\varepsilon_k^b \tag{34}$$

$$\bar{\varepsilon}_k^b = z_k - z_k(-) - N_k\bar{u}_k(-) = \bar{\varepsilon}_k^x - N_k\bar{u}_k(-) \tag{35}$$

$$P_{zz}^b = \sum_{i=0}^{2n} w_i\left(z_{i,k-1}(+) - z_k(-)\right)\left(z_{i,k-1}(+) - z_k(-)\right)^T + R_k + N_kP_k^{b*}(-)N_k^T \tag{36}$$

$$\bar{P}_{zz}^b = \lambda_k^b P_{zz}^b,\ \lambda_k^b \geq 1, \quad \bar{P}_{zz}^b = \frac{1}{M-1}\sum_{i=k-M+1}^{k}\bar{\varepsilon}_k^b\bar{\varepsilon}_k^{bT} \tag{37}$$

$$\lambda_k^b = \max\left\{1, \frac{1}{m}tr\left(\bar{P}_{zz}^b\left(P_{zz}^b\right)^{-1}\right)\right\} \quad \text{or} \quad \lambda_k^b = \max\left\{1, \frac{tr\left(\bar{P}_{zz}^b\right)}{tr\left(P_{zz}^b\right)}\right\} \tag{38}$$

with the coupling equations

$$N_k = \gamma_k H_k U_k, \quad U_k = \bar{U}_k\left(I - \lambda_k^b Q_{k-1}^b\left(\bar{P}_k^{b*}\right)^{-1}\right) \tag{39}$$

$$V_k = \bar{U}_k - \bar{K}_k^{b*}N_k, \quad \bar{U}_k = \left(\beta_k\Phi_{k-1}V_{k-1} + (I - \Gamma_{k-1})\right)r_{k-1}^{-1} \tag{40}$$

$$u_k = (\bar{U}_{k+1} - U_{k-1})\,\bar{r}_k \bar{u}_k(+), \quad \bar{Q}_k^x = Q_k^x + U_{k-1} Q_k^b \bar{U}_{k-1} \tag{41}$$

where

$$\Phi_k = \left(\frac{\partial f(x)}{\partial x}\bigg|_{x=\hat{x}_k} \right) \quad \text{and} \quad H_k = \left(\frac{\partial h(x)}{\partial x}\bigg|_{x=\hat{x}_k} \right) \tag{42}$$

Furthermore, the unknown instrumental diagonal matrices $\beta_k = \text{diag}(\beta_{1,k}, \beta_{2,k}, \ldots, \beta_{N,k})$ and $\gamma_k = \text{diag}(\gamma_{1,k}, \gamma_{2,k}, \ldots, \gamma_{N,k})$ are introduced in order to take these residuals into account and obtain a more exact equality.

Finally, the initial conditions are

$$\bar{x}_0(+) = x_0^* - V_0 u_0^*, \quad \bar{u}_0(+) = u_0^*, \quad V_0 = P_0^{b*} \left(P_0^b \right)^{-1} \tag{43}$$

$$\bar{P}_0^x = P_0^x - V_0 P_0^b V_0^T, \quad \bar{P}_0^b(+) = P_0^b \tag{44}$$

Equations (39) to (60) are used to design the reconfigurable controller.

5. SIMULATION RESULTS

The simulation results in the preceding two examples are as follows: One is a discretized microsatellite nonlinear system that is stabilized by input-to-state discrete-time controller. The other is one of the four thruster microsatellites which has failed the reconfiguration of fault-tolerant controller is utilized to compensate the primary controller by using the size of control effectiveness factor.

Considering Eq. (17), we design a nonlinear sampled-data controller based on Section 3 and an approximation of the plant:

$$x_{k+1} = x_k + T\left(f(x_k) + g_2(x_k)\,\tau_u^b(x_k) \right) = F_T^a\left(x_k, \tau_u^b \right) \tag{45}$$

The controllers are based on approximations (46) that assign the following dynamics:

$$\tau_u^b = -\frac{1}{T}\left(\left(-\omega_{ob}^b \times + C_o^b \omega_{io}^o \right)^{\times} J \left(-\omega_{ob}^b \times + C_o^b \omega_{io}^o \right) + \omega_{ob}^b \times C_o^b \omega_{io}^o \right) - \frac{1}{T} J \omega_{ob}^{bT} J \omega_{ob}^b \tag{46}$$

The simulation result of microsatellite on-orbit thruster failed, one of the four thrusters was out of order, fault detection and diagnosis to diagnose the fault and tolerant control reconfigure overcame the fault. We design reconfigurable controller relative control effectiveness factor based on two-stage Kalman algorithm. Figure 4(a) shows the time response of a body attitude as thruster 1 faults at time 4 sec and reconfigures at time 12 sec. As thruster 1 faults at time 4 sec and reconfigures at time 12 sec, the thruster command time response is shown in Fig. 4(b).

6. CONCLUSIONS

Integration fault detection and tolerant attitude control in micro-satellite propulsion mode application approach based on control effectiveness factor has been investigated in this paper. The proposed scheme is based on a two-stage Kalman filter for state and control effectiveness factor estimation, the statistical decisions for fault detection, diagnosis and activation of the controller reconfiguration, and the reconfigurable controller design based on an approximate discrete-time input-to-state stabilize problem. Design of these propulsion mode subsystems is carried out simulation. The proposed approach is capable of dealing with different types of actuator faults and different types of reference inputs, disturbances and random noises. Simulation results have demonstrated the validation and effectiveness of this solution.

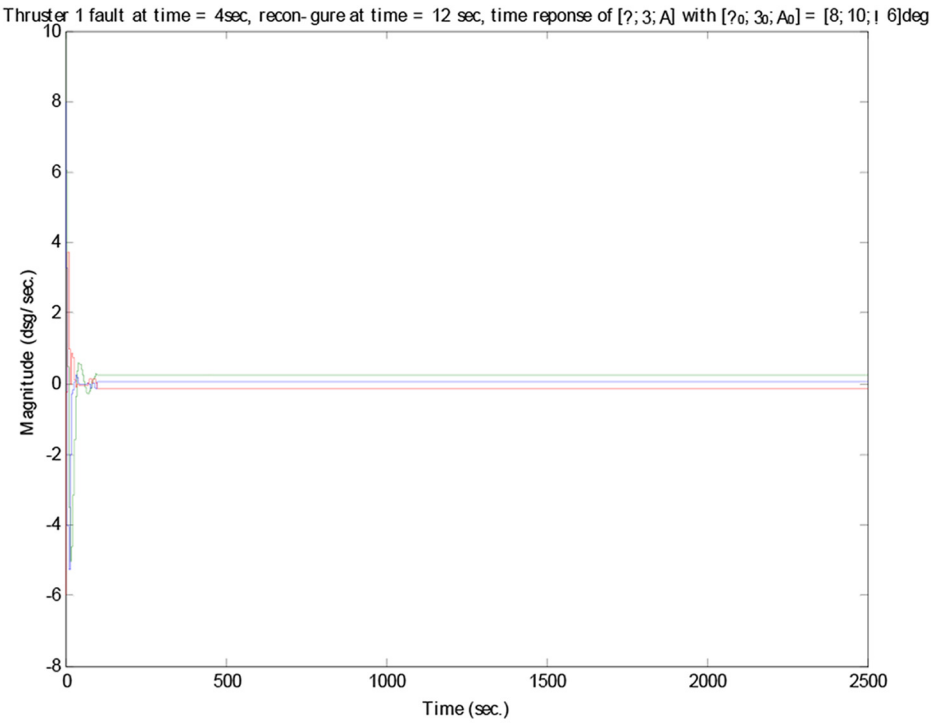

(a)

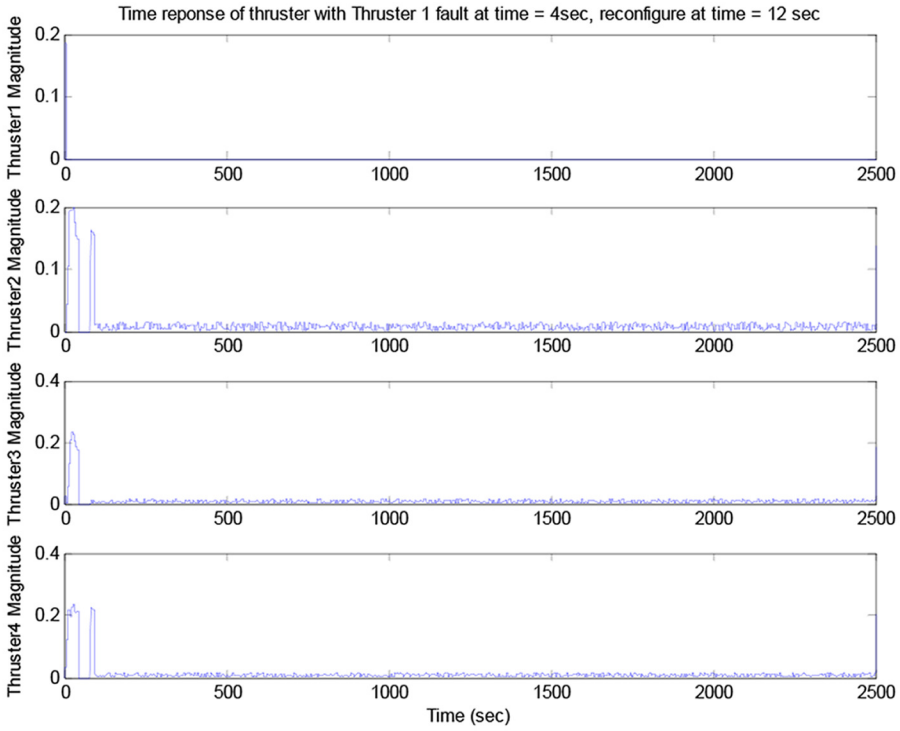

(b)

Fig. 4. (a) Time response of body attitude. (b) Time response of thrusters command.

ACKNOWLEDGEMENT

This work is supported by the ROC Ministry of Science and Technology under Contract No. MOST 104-2221-E-334-020 (academic research grants).

REFERENCES

1. Wu, N.E., Zhang, Y. and Zhou, K., "Detection estimation, and accommodation of loss of control effectiveness", *International Journal of Adaptive Control and Signal*, Vol. 14, pp. 775–795, 2000.
2. Huang, S., Tan, K.K., and Lee, T.H., "Fault diagnosis and fault-tolerant control in linear drives using the Kalman filter", *IEEE Transactions on Industrial Electronics*, Vol. 59, No. 11, pp. 4285–4292, 2012.
3. Nesica, D., Teelb, A.R. and Kokotovic, P.V., "Sufficient conditions for stabilization of sampled-data nonlinear systems via discrete-time approximations", *Systems & Control Letters*, Vol. 38, Nos. 4–5, pp. 259–270, 1999.
4. Nesic, D. and Laila, D.S., "A note on input-to-state stabilization for nonlinear sampled-data systems", *IEEE Transactions on Automatic Control*, Vol. 47, No. 7, pp. 1153–1158, 2002.
5. Wertz, J.R., *Spacecraft Attitude Determination and Control*, Kluwer Academic Publishers, 1978.
6. Shou, H.N., "Microsatellite attitude determination and control subsystem design and implementation", *Software-in-the-Loop Approach*, Vol. 2014, Article ID 904708
7. Hsieh, C.S., "Robust two-stage Kalman filters for systems with unknown inputs", *IEEE Transactions on Automatic Control*, Vol. 45, No. 12, pp. 2374–2378, 2000.